Dry mass grassland estimation using UAV ultra-wide RGB images

Rebeca Campos Emiliano da Silva [1], Antonio Maria Garcia Tommaselli [1], Nilton Nobuhiro Imai [1], Rorai Pereira Martins-Neto [2], Daniel da Silva da Silveira [3], Edemar Moro [3]

[1] Department of Cartography, São Paulo State University (UNESP) at Presidente Prudente, São Paulo, Brazil – (rebeca.campos, a.tommaselli, nilton.imai)@unesp.br
[2] Faculty of Forestry and Wood Sciences, Czech University of Life Sciences Prague, Kamycka 129, 16500 Prague, Czech Republic – pereira_martins_neto@fld.czu.cz
[3] University of Western São Paulo (UNOESTE) at Presidente Prudente, São Paulo, Brazil – dsilveira33@yahoo.com.br and edemar@unoeste.br

Keywords: grassland, dry matter, machine learning, UAV, precision agriculture, remote sensing.

Abstract

Dry mass is an important parameter to optimise grassland management. Traditionally, dry mass values are estimated manually by cutting, drying, and weighing vegetation samples. In large areas of cultivation, this becomes a time-consuming and costly activity. In recent years, many researchers have studied different sensors embedded in Unmanned Aerial Vehicles (UAV) to collect spatial data and estimate biomass using machine learning algorithms for forest and agricultural applications. However, there needs to be more research dealing with estimating production indices for pasture, especially in Brazil, as stated. This study evaluates the feasibility of using the GoPro wide-angle RGB camera on UAVs (Unmanned Aerial Vehicles) to estimate the dry mass of pastures. Different data analysis methods were compared, including the combination of vegetation indices (VIs) values and three-dimensional metrics (3D) extracted from the Canopy Height Model (CHM): all metrics (ALL), three VIs plus four 3D metrics (VI3 + CHM4) and only 3D metrics. Random Forest (RF) machine learning algorithm was used to estimate dry mass. The best results were obtained when merging all the variables from the two flight campaigns, with a coefficient of determination (R^2) of 0.80 for the model and a Pearson Correlation Coefficient (PCC) of 0.85 for validation, with a Root Mean Square Error (RMSE%) of 20.5%. In summary, using RGB sensors embedded in UAVs is a promising technique for estimating farm grazing parameters.

1. Introduction

Brazil is the world's leading beef exporter, occupying first place in the global ranking with more than 1.98 million tons (FAO 2022). Statistical data from ABIEC (2023) show that a large part of the herd, totalling 202 million head of cattle, was raised on the 154.5 million hectares used for pasture in the country (MAPBIOMAS, 2021), providing an average of 1.3 head per hectare. These figures suggest a concentration of a significant number of animals in a relatively restricted area, intending to optimize productivity.

Dry mass (DM), or dry matter, production refers to the amount of forage that remains after the removal of water through drying (Cardoso, 1996). Monitoring pasture DM production and spatial distribution plays a crucial role in pasture management, providing essential information for successful animal production, forage availability, nutritional quality, and effective management of natural resources (Mannetje, 2000; Silva and Cunha, 2003). Traditionally, DM values are estimated manually by cutting, drying, and weighing samples of the vegetation (Hopkins, 2000). In large areas of cultivation, this becomes a time-consuming and costly activity.

In recent years, the use of RGB, spectral and LiDAR sensors to collect spatial data and quantify relevant variables for agricultural, forestry and grassland monitoring applications has been widely studied (Moeckel et al., 2018; Lussem et al., 2022; Martins Neto et al., 2023). For farm applications, low-cost, lightweight RGB cameras coupled to Unmanned Aerial Vehicles (UAVs) have been used to acquire high spatial resolution data, although they have lower spectral resolution compared to multispectral cameras. Despite the RGB spectral limitations, these images can be used to calculate vegetation indices, improve the vegetation to background separation and minimise interference from light and target conditions (Zhang et al., 2022; Bazzo et al., 2023).

Photogrammetric image processing using Structure from Motion (SfM) techniques enables the generation of photogrammetric products and three-dimensional terrain models, making it possible to extract height metrics from these models that are correlated with biomass (Viljanen et al., 2018). In addition, the extraction of different three-dimensional (3D) and spectral metrics supports the estimation of dependent variables using Machine Learning (ML) models (Bendig et al., 2015, Viljanen et al., 2018, Morais et al., 2021).

In this context, the use of low-cost action cameras, such as the GoPro camera (GoPro, 2024), can be an alternative to expensive multi- and hyperspectral sensors. This action camera can be advantageous due to its affordable cost, ease of use, ultrawide field of view, lightweight, high image resolution, and portability in mobile mapping systems and UAVs.

Nowadays, there is a lack of research addressing the estimation of production indices for grazing, especially in Brazil, as stated by Bazzo et al. (2023). In this context, the aim of this study is to assess the performance of an action camera, like GoPro, to estimate dry mass in grass areas, considering only normalized vegetation indices and canopy height metrics (CHM) generated from RGB images. The research aims to assess the feasibility of using affordable and widely available equipment to measure dry mass and optimize grassland management practices on a farm scale.

This contribution has been peer-reviewed. The double-blind peer-review was conducted on the basis of the full paper.
https://doi.org/10.5194/isprs-annals-X-3-2024-69-2024 | © Author(s) 2024. CC BY 4.0 License.

2. Study area and data acquisition

The study area is located on an experimental farm, in the Nova Pátria district, municipality of Presidente Bernardes, São Paulo state, Brazil (22°17'4.85"S, 51°40'46.31"W) (Figure 1). The flight campaigns were carried out on January 18 and March 27, 2021, with a flight height of 80 m above the ground. The RGB images were acquired with a GoPro Hero4 Black super-wide-angle action camera (Table 1) onboard a Quadcopter UAV, model UX4 (Nuvem UAV). The bundle block adjustment of the images was performed with a set of eight Ground Control Points (GCPs), whose planialtimetric coordinates were measured with a double frequency GNSS receiver.

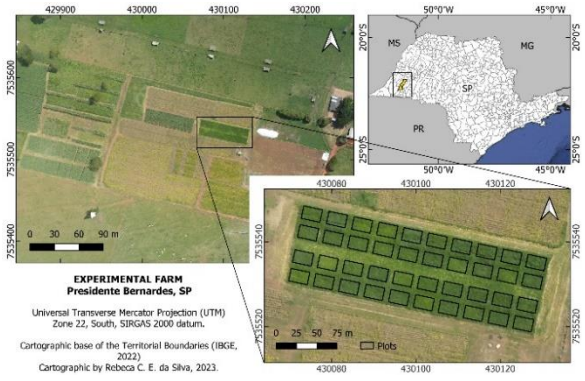

Figure 1. Location of the grass plots at Unoeste Experimental Farm, Presidente Bernardes, SP, Brazil.

Camara details	Specifications
Model	GoPro HERO4 Black
Focal length	3 mm
Pixel size	1.73 × 1.73 µm
Image size	4000 × 3000 pixels
Sensor	6.17 × 4.55mm CMOS
Dimensions	41 mm × 59 mm × 30 mm
Weight	152 g
Image format	JPEG

Table 1. GoPro Camera specifications.

The ground reference samples were acquired and provided by researchers from the University of Western São Paulo (Unoeste). The experiment was conducted in an area with 40 plots (dimensions of 3.5 × 5.0 m each) of grass, composed of the species *Urochloa Brizantha* (syn. *Brachiaria brizantha*), with chemical treatments at nitrogen (0, 150, 300, 450, 600 kg/ha) with and without sulfur with four repeats per treatment. An area of 0.5 m² (dimensions of 1.0 × 0.5 m) of grass per plot was cut using a metal rectangle as a field reference sample. The samples were then dried and weighed to calculate the dry mass in kg/ha units, on two separate dates. Table 2 shows the mean weight and standard deviation of the grass samples.

Sampling date	Mean (kg/ha)	Std (kg/ha)
11/01/2021	2601.35	513.21
29/03/2021	4740.53	1276.07

Table 2. First cut (11/01/2021) and second cut (29/03/2021) data mean, standard deviation (Std).

3. Methodology

3.1 Geometric processing

The image datasets for each date were processed individually using bundle block adjustment in the Agisoft software, version 1.8.4 (Agisoft LLC 2022). The settings for each project were defined with a fixed standard deviation of 10 m for the camera stations coordinates components (E, N, h) and 30° for the attitude angles, since no accurate geotagging system was available; the GCPs (two checkpoints and six control points) were set with a standard deviation of 5 mm. The photogrammetric projects for the two dates were set for the WGS84 reference system and UTM projection, zone 22, with an average flight height of 80 m, with a measurement error of 1 px, and a fisheye camera model.

Image processing followed the general phototriangulation workflow: (1) started with image matching and initial alignment, resulting in a sparse point cloud; (2) insertion of the six ground control points and two check points for bundle adjustment and estimation of the camera's interior and exterior orientation parameters based on the control points; (3) manual filtering of the point cloud to remove outliers; (4) refinement of the bundle adjustment; and (5) generation of the dense point cloud with mild filtering, using estimated exterior and interior orientation. The digital surface model (DSM) is then created from the dense point cloud, including terrain and above-ground object information. Orthomosaics were generated from the image projections and their orientation and DSM parameters and exported at 5 cm GSD (Ground Sample Distance) for both datasets.

To generate the digital canopy height models (CHMs) of the grass, the procedure of Oliveira et al.(2020) was adopted, which involves the automatic classification of ground points using specific input parameters. Due to the variation in grass height, manual adjustments were necessary to correct regions that were not correctly identified. After classification, digital terrain models (DTMs) were generated with standard interpolation and exported in TIFF format with a GSD of 10 cm. CHMs were created using QGIS software, version 3.34.35 (QGIS Development Team, 2023), applying the difference between the DSM and the DTM.

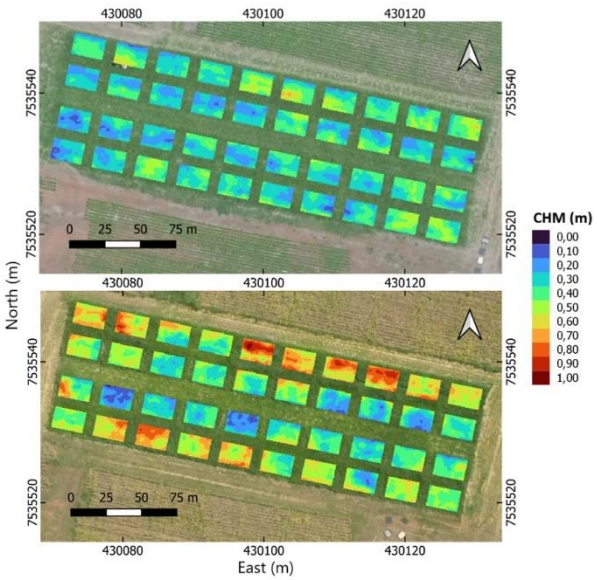

Figure 2. Canopy Height Models (CHM) of the grass on January 18 (a) and March 27, 2021 (b).

Figure 2 shows the CHM from the two epochs, with a different color symbol used to represent the variations in vegetation height in the 0-1 m range. It can be observed that the spatial distribution of the grass is not homogeneous within each plot. The CHM for March 27, 2021 showed larger height values.

Finally, the statistics of the control and check points were analyzed, such as standard deviation (σ) and RMSE (Root Mean Square Error), to verify and evaluate the quality of the results.

3.2 RGB vegetation indexes and 3D metrics

Only RGB-based vegetation index (VIs) values were used as input data, (Table 3) based on the three bands of the visible spectrum, like the Grassland Index (GrassI), Green Leaf Index (GLI), Normalized Green Red Difference Index (NGRDI), Plant Pigment Ratio Index (PPRI) and Red Green Blue Vegetation Index Excess (RGBVI). These indices have already been tested in priveous studies to estimate biomass with UAV images (Bendig et al., 2015; Bareth et al., 2015; Viljanen et al., 2018; Lussem et al., 2019, 2022). All indices were calculated using the raster calculator in QGIS software, version 3.34.35 (QGIS Development Team 2023).

Equation	Reference
$GrassI = RGBVI + CHM$	(Bareth et al., 2015)
$GLI = \frac{2G - R - B}{2G + R + B}$	(Gobron et al., 2000)
$\mathrm{NGRDI} = \frac{\mathrm{G} - \mathrm{R}}{\mathrm{G} + \mathrm{R}}$	(Tucker, 1979)
$\mathrm{PPRI} = \frac{\mathrm{G} - \mathrm{B}}{\mathrm{G} + \mathrm{B}}$	(Metternicht, 2003)
$RGBVI = \frac{G^2 - (R * B)}{G^2 + (R * B)}$	(Bendig et al., 2015)

Table 3 – Vegetation Indices for RGB images.

Furthermore, eight three-dimensional (3D) metrics were calculated for the CHMs (Table 4). The 3D metrics were computed using a script implementation in R, version 4.3.2 (R Core Team, 2023).

CHM metrics	Equation
Maximum height	$CHM_{max} = max(h_i)$
Minimum height	$CHM_{min} = min(h_i)$
Mean height	$CHM_{mean} = \frac{1}{N}\sum_{i=1}^{N} h_i$
Median height	$CHM_{median} = \begin{cases} if\ unpaired: h_{\left(\frac{N+1}{2}\right)} \\ if\ pair: \frac{\left(h_{\left(\frac{N+1}{2}\right)} + h_{\left(\frac{N}{2}\right)}\right)}{2} \end{cases}$
Standard deviation heigh	$CHM_{std} = \sqrt{\frac{\sum_{i=1}^{N}\left(h_i - \bar{h}\right)^2}{N-1}}$
(30, 60, 90)th percentile	$CHM_{p30,60,90} = \frac{\left(\left(\frac{p}{100}\right) * (N+1)\right)}{100}$

Table 4 – 3D metrics derived from the CHM.

3.3 Feature extraction process

As the field reference values for the grass are not georeferenced, it was essential to analyze the spatial distribution of the grass and identify the areas with the highest plant density in order to extract the Vegetation Index (VI) values and 3D metrics for each plot. To achieve this, a stack file was generated in which the pixels refer to the regions with the highest VIs and CHM values in each plot, following the procedure described below and accomplished in QGIS:

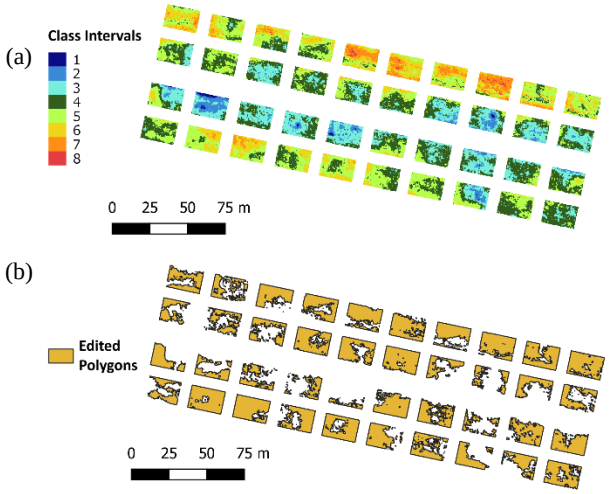

Figure 3. (a) Reclassified parcels’ image and (b) SHP_{class} edited for March 27, 2021.

(1) Creation of a shapefile delimiting the 40 plots, each with dimensions of 3 × 4.5 m. A buffer of approximately 25 cm was excluded to avoid edge effects around the plots;
(2) Clipping the GrassI index images ($GrassI_{rec}$) with the plot delimitation shape using the “clipping raster by extension tool”;
(3) Evaluation of the data distribution and definition of the number of classes. In that instance, the Sturges (1926) method was applied to the field reference values for the dry mass of the grass from the two dates together, resulting in approximately seven classes. However, we opted for eight class intervals based on the classification of the $GrassI_{rec}$ image from March 27, using the equal interval interpolation method, in order to better capture the data values distributions;
(4) Slicing the GrassIrec index image, for each date, considering the eight equal class intervals with the GRASS plugin's "r.recode" reclassification tool (Figure 3.a);
(5) Creation of the polygon shapes (SHP_{class}) based on the reclassified images using the "raster to vector" tool in the GDAL plugin;
(6) Editing the SHP_{class} by removing the polygons with the lowest class values from each plot. During this stage, each plot was visually inspected, retaining only two or three polygons with the highest class values (Figure 3.b);
(7) Merging the remaining adjacent SHP_{class} polygons with the "dissolve" tool. Thus, the polygons of each plot refer to the boundaries of the regions with the highest grass growth, even for the sparsest plot;

(8) Creating a raster with the IDs of each plot;
(9) Stacking the rasters with the plot IDs, the five VIs and the CHM in a single file for each date. The CHM was resampled to 5 cm to make it compatible with the VI images;
(10) Clipping the stack files with the SHP_{class} for each date. As a result, a stack is obtained with the VIs and CHM images delimited to the highest class values.

With this final stack for each date, the means of the VIs values for the highest class values were calculated per plot, totalling 200 samples of VI values. In addition, the CHM metrics were calculated using the heights corresponding to the highest class values, specified by the equations shown in Table 4, a total of 320 3D values. The 3D and VIs features were obtained using a script implemented in R.

3.4 Regression model and quality assessment

The statistical analysis and modelling steps were carried out using R, with the Caret (Kuhn, 2008) and Random Forest (Breiman, 2001) packages. Given the small size of the data set, with only 40 samples, the data was randomly divided into 70 % of the samples for training and 30 % of the samples for validation.

The modelling was performed using the Random Forest algorithm, calibrated using the repeated cross-validation method (repeatedcv). Random Forest, developed by Breiman (2001), is a machine learning technique for classification and regression analysis which combines several independent decision trees. This approach reduces the correlation between trees and minimizes overfitting problems.

Repeated cross-validation with Random Forest involves performing cross-validation with 10 iterations, each with 5 repetitions. This means that the model is tested on different subsets of the dataset, in different combinations, and repeated to ensure more robust and reliable results. The average of the performance metrics across all repetitions provides a more accurate estimate of the model’s performance.

When using RF, there is no need to make a selection of characteristics, as the calculations include measures of the order of importance of these characteristics (Näsi et al., 2018). However, to assess the correlation and contribution of the variables to predicting dry mass, Pearson's correlation matrix and principal component analysis (PCA) were calculated for the dataset. Regression models were then tested in three different contexts: using the data set from each date separately and combining the two merged sets. These models were developed using the variables identified in the cross-validation, the 3D metrics, and the combination of three vegetation indices with four 3D metrics (VI_3 + CHM_4).

The models were evaluated based on the following parameters: coefficient of determination (R^2), root mean square error (RMSE), and percentage root mean square error (RMSE%). The Pearson correlation, RMSE, and RMSE% metrics were used to analyze the models' validation.

4. Results

4.1 Geometric processing analysis

The RMSE values for each component of the check points after bundle adjustment (Table 5) indicate that the photogrammetric processing obtained satisfactory results, with errors with a magnitude of centimetres. The RMSE for the planimetric coordinates (X, Y) ranged from 0.19 to 1.65 cm, while the maximum error for the altimetric component (Z) was 0.88 cm. The total RMSE of the points in the images was 0.04 pixels on both dates.

Date	$X_{(cm)}$	$Y_{(cm)}$	$Z_{(cm)}$	$3D_{(cm)}$	$Image_{(px)}$
03/27/2021	0.19	0.68	0.88	0.42	0.04
01/18/2021	0.22	1.65	0.02	0.53	0.04

Table 5. RMSE of the check points.

In terms of processing, the March 27 campaign used 147 images, while the January 18 campaign used 157 images, and the reprojection error was 1.15 pixels in March and 1.1 pixels in January. At the end of the geometric processing, the dense point clouds were used to reconstruct the DSMs, with a point density of 130 points/m² for January 18, 2021, and 123 points/m² for March 27, 2021.

4.2 Correlation analysis and variables contribution

The relationships between the variables are depicted in the bivariate linear correlation graph (Figure 4), in which the correlation values between the variables are indicated by colours: negative correlations (red) and positive correlations (blue). The correlation coefficient is proportional to the intensity and size of the circle. As expected, dry mass showed a strong correlation with the 3D metrics and with the GrassI index, also calculated with the CHM. Only the NGRDI index showed a weaker correlation compared to the independent variables, with a moderate but negative correlation value. The other VIs showed a moderate and positive correlation with dry mass.

Figure 5 shows the results of the principal component analysis expressed as a vector graph, in which the contribution of each component (dimension) is represented by the direction and length of the vectors. The length of the vector indicates the magnitude of each variable's contribution, while the direction of the vector indicates the influence of each variable on the respective component. The first component explained 68.7% of the total variance present in the data with the greatest contribution from the GrassI index and the following 3D metrics: CHM_{p90}, CHM_{max}, CHM_{p60}, CHM_{mean}, CHM_{median} and CHM_{p30}. The second component explained 20.8% of the total variance.

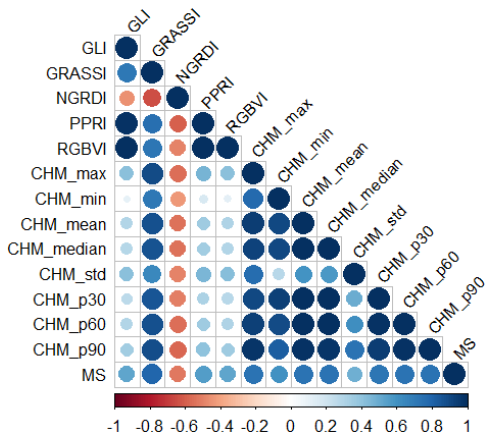

Figure 4. Correlation matrix calculated using the Pearson correlation coefficient.

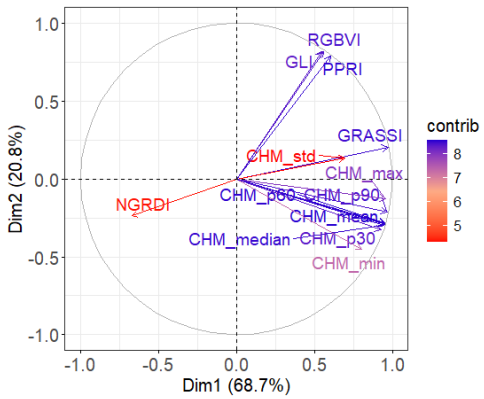

Figure 5. Projection of features for the first and fourth principal components and their contributions.

4.3 Regression model

The results of the training (Table 6) and validation (Table 7) models for estimating dry mass showed different levels of performance based on the variables used in each data set. Models were tested that included all the variables (ALL), models that used only the 3D metrics (CHM_{all}), and models that considered the correlation of the variables together with empirical tests (VI_3 + CHM_4). In the VI_3 + CHM_4 sample set, the GrassI, PPRI and RGBVI indices were adopted, with the 3D metrics CHM_{min}, CHM_{mean}, CHM_{p30} and CHM_{p60}.

For the training models for the January 18, 2021 dataset, the model fitted/produced with the VI_3 + CHM_4 combination obtained an R^2 of 0.65, indicating better performance than the other combinations, although with an RMSE of 516.48 kg/ha. For the March 27, 2021 dataset, there was a significant improvement in the overall performance of the models. The model with VI_3 + CHM_4 variables had the best performance, with an R^2 of 0.77 and an RMSE of 965.74 kg/ha. In both tests, the models incorporating all variables (ALL) exhibited the lowest RMSE.

For the merged data set, the results indicated that the VI_3 + CHM_4 combination also achieved the best performance, with an R^2 of 0.80 and an RMSE of 747.24 kg/ha. The model ALL obtained a similar R^2 of 0.80, but with an RMSE of 798.12 kg/ha, while the model with only CHM_{all} variables performed worse, with an R^2 of 0.66 and the highest RMSE of 1009.31 kg/ha.

Date	Variable	R^2	RMSE (kg/ha)
01/18	ALL	0.5437	492.10
	CHM_{all}	0.5157	526.75
	VI_3 + CHM_4	0.6531	516.48
03/27	ALL	0.6889	935.17
	CHM_{all}	0.6853	993.66
	VI_3 + CHM_4	0.7771	965.74
Fusion	ALL	0.8033	798.12
	CHM_{all}	0.6552	1009.31
	VI_3 + CHM_4	0.8046	747.24

Table 6. Coefficient of determination (R^2) and RMSE for dry mass (DM) training model.

For the model validation of the January 18, 2021 dataset, the VI_3 + CHM_4 combination obtained a PCC of 0.7445, RMSE of 467.31 kg/ha and percentage RMSE of 19.16%, indicating a better performance than the other isolated variables. However, CHM_{all} model had the lowest RMSE. For the March 27, 2021 dataset, the same combination also showed the best performance, with a PCC of 0.7531, RMSE of 872.76 kg/ha and RMSE% of 18.25%.

For the merged data set, the results indicate that the ALL combination performed best, with a PCC of 0.85, RMSE of 773.74 kg/ha and percentage RMSE of 20.53%. The model with CHM_{all} variables showed the worst performance with an RMSE% of 28.17%.

The models with the merged data obtained the best results. Figure 6 shows the normalized relative importance values from 0 to 100 for the variables in the different training models for the merged data set. In this case, the GrassI and PPRI variables were more relevant in the ALL and VI_3 + CHM_4 models, while the CHM_{media} and CHM_{mean} variables were more relevant in the model with the CHM_{all} metrics.

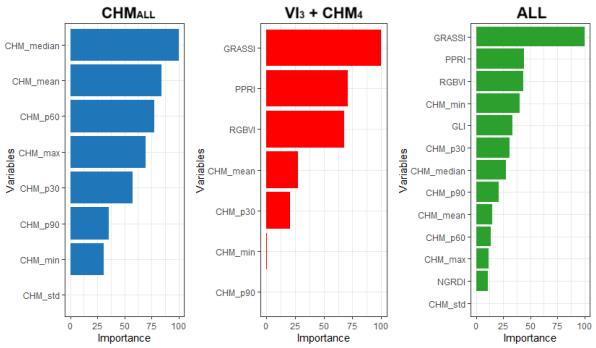

Figure 6. Importance of the variables in the training model for the fused dataset.

In general, the models with the combination of VI and 3D metrics had the best performance, with the highest PCC and the lowest RMSE and percentage RMSE, especially for the merged data set. This suggests that the combination of these variables is more effective in estimating dry mass than using the single variables.

Date	Variable	PCC	RMSE (kg/ha)	RMSE%
01/18	ALL	0.6213	439.68	16.77
	CHM_{all}	0.5968	521.66	22.19
	VI_3 + CHM_4	0.7745	467.31	19.16
03/27	ALL	0.7579	1076.26	21.67
	CHM_{all}	0.6536	1106.34	22.75
	VI_3 + CHM_4	0.7531	872.76	18.25
Fusion	ALL	0.8460	773.74	20.53
	CHM	0.6413	977.99	28.17
	VI_3 + CHM_4	0.8492	822.29	23.63

Table 7. Pearson Correlation Coefficients (PCC), Root mean squared error (RMSE) and RMSE% for dry mass (DM) validation model.

This contribution has been peer-reviewed. The double-blind peer-review was conducted on the basis of the full paper.
https://doi.org/10.5194/isprs-annals-X-3-2024-69-2024 | © Author(s) 2024. CC BY 4.0 License.

5. Discussion

In the experiment, the combination of spectral and non-spectral data extracted from RGB images was used to estimate dry mass. To minimize for illumination variations between the images and enhance the contrast between vegetation areas and other surfaces, RGB indices based on normalized differences were considered. In addition, canopy height model metrics were derived directly from the image sets themselves.

Due to the lack of georeferencing of the field samples and to avoid bias in the data, it was decided to use the highest values of the vegetation index to calculate the average vegetation indices (VIs) and 3D metrics. This made it impossible to automatically extract point attributes, as observed in other studies. In addition, grass growth was not uniform across all the plots. In the CHM generated with images collected on January 18th, it is possible to notice the low growth of the grass, reaching a maximum height of 0.64 m. This was expected, as the grass had been cut prior to January. However, for the CHM generated with images collected on March 27th, the grass showed significant growth, reaching a maximum height of 0.96 m. This increase is natural and expected during the rainy season from January to March.

Comparing the regression results with other pasture dry mass estimation studies using RF, it was observed that Viljanen et al. (2018) reported a PCC of 0.77, which was obtained with RGB channel attributes alone and a PCC of 0.96 when combining RGB + 3D values, sampled from 96 plots. Näsi et al. (2018) achieved a PCC of 0.10 using only 3D metrics and a PCC of 0.63 for VI and 3D values, when estimating dry mass from a set of 8 field reference samples. Morais et al. (2021) evaluated the use of different machine learning algorithms to estimate pasture biomass; they concluded that Multiple Regression Analysis (MLR) had the highest median R^2 of 0.76, followed by partial least squared regression (PLSR) with R^2 of 0.75 and RF with R^2 of 0.69. Therefore, the accuracy of the analysis may depend more on the quantity and quality of the field samples rather than on the regression algorithm (Morais et al., 2021, Bazzo et al., 2023).

Among the indices used, GrassI, based on RGBVI, and PPRI stood out as relevant variables for predicting grass dry mass. To the best of our knowledge, PPRI was only tested in Lussem (2022), where it was considered the most important variable for predicting N content in grass. The RGBVI uses RGB data to highlight areas of vegetation, while the Grassland Index incorporates 3D metrics from the CHM. Unlike the results of Bendig et al. (2015), the RGBVI index was one of the most relevant variables for the model. Such a combination provides a more robust estimate by offering greater sensitivity to changes in vegetation in the early stages of growth as shown by Bareth et al. (2015).

6. Conclusions

The study assessed the effectiveness of using RGB images acquired by an action camera mounted on a UAV to estimate dry mass in a grass area using machine learning techniques. 3D data was extracted from photogrammetric canopy height models generated from photogrammetric point clouds, while normalized vegetation index images were derived from RGB information.

Data from individual campaigns was not sufficient to accurately estimate dry mass from images only. However, combining RGB data and 3D metrics from two separate campaigns resulted in improved performance. Other studies integrating RGB and 3D data, combining different acquisition dates, have shown similar or superior results using multi- and hyperspectral cameras (Viljanen et al., 2018; Lussem et al., 2022; Bazzo et al., 2023). Regression models generated from images acquired on different dates allow for a more comprehensive and robust evaluation compared to using data from a single date. This approach can enhance the precision and reliability of estimates when the models are applied for inference on other dates.

It is important to put these results in perspective, since RGB cameras have advantages for small-scale agriculture, offering a cost-effective solution for farm monitoring. To the best of our knowledge, this study is the first to use a wide-angle action camera for this application, contributing to the advancement in the use of RGB photogrammetry techniques in agricultural areas. The sampling method, which involved using the highest values from the largest classes of the vegetation index in each plot, can be compared in the future with other techniques, such as pixel-by-pixel or area sampling, to evaluate their contribution to the model. It is also suggested to compare this methodology with other sensors, like multispectral and hyperspectral lightweight cameras.

Acknowledgements

This study was financed in part by the Coordenação de Aperfeiçoamento de Pessoal de Nível Superior – Brasil (CAPES) (88887.310313/2018-00 and 88887.898553/2023-00), by the National Council for Scientific and Technological Development, CNPq (grants n. 130411/2022-1 and 303670_2018-5]) and by the São Paulo Research Foundation, FAPESP (Grant: 2021/06029-7).

References

ABIEC, Associação Brasileira das Indústrias Exportadoras De Carne. 2023. *Beef Report 2023: A pecuária do Brasil*. ABIEC, Brasília, 110.

Agisoft LLC. 2022. Agisoft Metashape software. https://www.agisoft.com/ (1 January 2024).

Bareth, G., Bolten, A., Hollberg, J., Aasen, H., Burkart, A., Schellberg, J. 2015. Feasibility study of using non-calibrated UAV-based RGB imagery for grassland monitoring: Case study at the Rengen Long-term Grassland Experiment (RGE), Germany. : 55–62.

Bazzo, C.O.G., Kamali, B., Hütt, C., Bareth, G., Gaiser, T. 2023. A Review of Estimation Methods for Aboveground Biomass in Grasslands Using UAV. *Remote Sensing* 15: 639.

Bendig, J., Yu, K., Aasen, H., Bolten, A., Bennertz, S., Broscheit, J., et al. 2015. Combining UAV-based plant height from crop surface models, visible, and near infrared vegetation indices for biomass monitoring in barley. *International Journal of Applied Earth Observation and Geoinformation* 39: 79–87.

Breiman, L. 2001. Machine Learning. *randomForest: Breiman and Cutler’s Random Forests for Classification and Regression* 45: 5–32.

Cardoso, E.G. 1996. *Engorda de bovinos em confinamento (Aspectos gerais). - Portal Embrapa*. In: *EMBRAPA-CNPGC*. EMBRAPA-CNPGC, Campo Grande, MS, 36p.

FAO. 2022. Food and Agriculture Organization of the United Nations. .

GoPro. 2024. *GoPro Hero4 Black*. https://gopro.com/pt/br/ (19 April 2024).

Hopkins, A. 2000. *Grass: its production and utilization*. In: Hopkins, A. (Ed.) 3rd ed ed. Published for the British Grassland Society by Blackwell Science, Oxford , Malden, MA, 440p.

Kuhn, M. 2008. Building Predictive Models in R Using the caret Package. *Journal of Statistical Software* 28.

Lussem, U., Bolten, A., Menne, J., Gnyp, M.L., Schellberg, J., Bareth, G. 2019. Estimating biomass in temperate grassland with high resolution canopy surface models from UAV-based RGB images and vegetation indices. *Journal of Applied Remote Sensing* 13: 1.

Lussem, U., Bolten, A., Kleppert, I., Jasper, J., Gnyp, M.L., Schellberg, J., et al. 2022. Herbage Mass, N Concentration, and N Uptake of Temperate Grasslands Can Adequately Be Estimated from UAV-Based Image Data Using Machine Learning. *Remote Sensing* 14: 3066.

Mannetje, L. 2000. Measuring biomass of grassland vegetation. In: Mannetje, L., Jones, R.M. (Eds.), *Field and Laboratory Methods for Grassland and Animal Production Research*, 1st ed.CABI Publishing, UK, p.151–177.

Martins Neto, R.P., Tommaselli, A.M.G., Imai, N.N., Honkavaara, E., Miltiadou, M., Saito Moriya, E.A., et al. 2023. Tree Species Classification in a Complex Brazilian Tropical Forest Using Hyperspectral and LiDAR Data. *Forests* 14: 945.

Moeckel, T., Dayananda, S., Nidamanuri, R., Nautiyal, S., Hanumaiah, N., Buerkert, A., et al. 2018. Estimation of Vegetable Crop Parameter by Multi-temporal UAV-Borne Images. *Remote Sensing* 10: 805.

Morais, T.G., Teixeira, R.F.M., Figueiredo, M., Domingos, T. 2021. The use of machine learning methods to estimate aboveground biomass of grasslands: A review. *Ecological Indicators* 130: 108081.

Näsi, R., Viljanen, N., Kaivosoja, J., Alhonoja, K., Hakala, T., Markelin, L., et al. 2018. Estimating Biomass and Nitrogen Amount of Barley and Grass Using UAV and Aircraft Based Spectral and Photogrammetric 3D Features. *Remote Sensing* 10: 1082.

Oliveira, R.A., Näsi, R., Niemeläinen, O., Nyholm, L., Alhonoja, K., Kaivosoja, J., et al. 2020. Machine learning estimators for the quantity and quality of grass swards used for silage production using drone-based imaging spectrometry and photogrammetry. *Remote Sensing of Environment* 246: 111830.

QGIS Development Team. 2023. QGIS Geographic Information System. Open Source Geospatial Foundation Project. http://qgis.osgeo.org (1 January 2024). .

R Core Team. 2023. The R Project for Statistical Computing. https://www.r-project.org/ (19 April 2024). .

Silva, S.C.D., Cunha, W.F.D. 2003. Métodos indiretos para estimar a massa de forragem em pastos de Cynodon spp. *Pesquisa Agropecuária Brasileira* 38: 981–989.

Sturges, H.A. 1926. The Choice of a Class Interval. *Journal of the American Statistical Association* 21: 65–66.

Viljanen, N., Honkavaara, E., Näsi, R., Hakala, T., Niemeläinen, O., Kaivosoja, J. 2018. A Novel Machine Learning Method for Estimating Biomass of Grass Swards Using a Photogrammetric Canopy Height Model, Images and Vegetation Indices Captured by a Drone. *Agriculture* 8: 70.

Zhang, H., Tang, Z., Wang, B., Meng, B., Qin, Y., Sun, Y., et al. 2022. A non-destructive method for rapid acquisition of grassland aboveground biomass for satellite ground verification using UAV RGB images. *Global Ecology and Conservation* 33: e01999.